

binding activity. The reaction was started by adding membranes containing human S1P<sub>1</sub>, S1P<sub>2</sub>, S1P<sub>3</sub> or S1P<sub>5</sub> receptors to the assay buffer including S1P (0.1 μM) and the desired concentration of TY-52156 (TY)(μM). The results are representative of three or four independent experiments. The relative percentage compared with the vehicle was calculated and expressed as mean±S.E.M. C, S1P<sub>1</sub>-, S1P<sub>2</sub>- or S1P<sub>3</sub>-CHO were pretreated with vehicle, TY-52156 (TY) (10 μM), VPC23019 (VPC) (10 μM) or JTE013 (JTE) (1.0 μM) for 10 min, and then treated with vehicle or S1P (0.1 μM) to determine p44/p42 MAPK phosphorylation. D, The data obtained from three independent experiments in C were quantitatively analyzed. ## *P*<0.01 vs S1P alone in S1P<sub>1</sub>-CHO, ++ *P*<0.01 vs S1P alone in S1P<sub>2</sub>-CHO, \* *P*<0.05 vs S1P alone in S1P<sub>3</sub>-CHO (Dunnett's test).

### Fig. 3

Effects on the S1P- or U46619-induced change in cardiac coronary flow in isolated perfused rat hearts. A and B, Isolated rat hearts were perfused at 37°C in a Langendorff manner with Krebs-Henseleit bicarbonate buffer at a constant perfusion pressure (70±5 mmHg). A, S1P dose-dependently (0.001 or 0.1 μM) decreased CF. Results are representative of five independent experiments. \*\* *P*<0.01 vs vehicle (Dunnett's test). B, Perfused rat hearts were pretreated with TY-52156 (TY) (0.1 μM), VPC23019 (VPC) (0.1 μM) or JTE013 (JTE) (0.1 μM) for 10 min, and then treated with vehicle, S1P (0.1 μM) or U46619 (0.1 μM). Results are representative of five independent experiments. \*\* *P*<0.01 vs S1P alone (Dunnett's test).

### Fig. 4

Effects of TY-52156 on the S1P-induced contractile response in isolated canine cerebral arteries. A, S1P dose-dependently (0.1 to 10  $\mu\text{M}$ ) induced vasoconstriction in isolated canine cerebral arteries. Results are representative of three independent experiments. B, Canine cerebral arteries were contracted by S1P (5.0  $\mu\text{M}$ ). After the maximum contractile response was observed, an increasing amount of TY-52156 (up to 10  $\mu\text{M}$ ) was applied to the organ chambers. Relaxation responses were measured every 10 min after addition of the indicated concentration of vehicle or TY-52156 ( $\mu\text{M}$ ). Results are representative of four independent experiments. \*  $P < 0.05$ , vs indicated dose of vehicle (Student's t-test).

Fig. 5

Effects of S1P receptor antagonist on S1P-induced Rho activation in HCASMCs. HCASMCs were pretreated with vehicle or the indicated concentration ( $\mu\text{M}$ ) of test the drug for 10 min, and further treated with vehicle, S1P (1.0  $\mu\text{M}$ ) or SEW2871 (SEW) (10  $\mu\text{M}$ ) for 3 min. The data obtained from three (A, B, D) or four (C) independent experiments were quantitatively analyzed (bottom panels). \*  $P < 0.05$ , vs S1P alone (Dunnett's test).

Fig. 6

Effects of S1P receptor antagonist on the S1P-induced increase in  $[\text{Ca}^{2+}]_i$  in HCASMCs. HCASMCs were pretreated with vehicle or the indicated concentration ( $\mu\text{M}$ ) of the test drug for 20 min, and further treated with vehicle, or S1P (0.01  $\mu\text{M}$ ). Results are representative of three or four independent experiments. The relative percentage compared with the vehicle was calculated and expressed as mean  $\pm$  S.E.M. \*  $P < 0.05$ ,

vs S1P alone (Dunnett's test).

Fig. 7

Effects of TY-52156 on FTY-720-induced bradycardia and hypertension in SD rat.

A. The oral bioavailability of TY-52156 was studied in SD rats. The plasma concentration of TY-52156 was determined by LC/MS/MS. Area under the blood concentration curve (AUC) from zero to 360 min was calculated using a trapezoidal rule. The results are expressed as mean±S.D. B, The plasma concentration of TY-52156 after oral administration was determined by LC/MS/MS. The dose of TY-52156 (TY) was 10 (*open triangle*) or 30 mg/kg (*closed triangle*). The results are expressed as mean±S.D. for three SD rats. C and D, Changes in HR (C) and SBP (D) were recorded after the oral administration of TY-52156 (TY) (10 mg/kg; *open triangle*; or 30 mg/kg; *closed triangle*) or control (*open circle*) in conscious rats. Results are representative of five independent experiments. E and F, Changes in HR (E) and MBP (F) were recorded after the administration of FTY-720 (1.0 mg/kg i.v.; *closed circle*) or control (*open circle*) in anesthetized rats. TY-52156 (TY) (10 mg/kg; *open triangle*; or 30 mg/kg; *closed triangle*) was administered orally at 4 h prior to FTY-720 injection. Results are representative of six independent experiments. \*  $P < 0.05$  vs control (unpaired Student's t-test). #  $P < 0.05$  vs FTY-720 alone (Dunnett's test).

Fig. 8

Effects of TY-52156 on the FTY-720-P-induced increase in  $[Ca^{2+}]_i$  in S1P<sub>3</sub>-CHO. S1P<sub>3</sub>-CHO were pretreated with vehicle or the indicated concentration ( $\mu$ M) of TY-52156 (TY) for 20 min, and further treated with vehicle or FTY-720-P (0.5  $\mu$ M).

MOL#61481

The results are representative of five independent experiments. The ratio of the fluorescence intensity was calculated. The relative percentage compared with the vehicle was calculated and expressed as mean±S.E.M. \*  $P < 0.05$ , vs FTY-720-P alone (Dunnett's test).

Fig. 9

Summary of signaling pathways for S1P-induced vasoconstriction. S1P causes vasoconstriction in smooth muscle cells via S1P<sub>2</sub> and S1P<sub>3</sub> receptors. Inhibition of both the increase in  $[Ca^{2+}]_i$  and Rho activation contributes to the efficacy of TY-52156 against S1P-induced vasoconstriction.

Fig.1

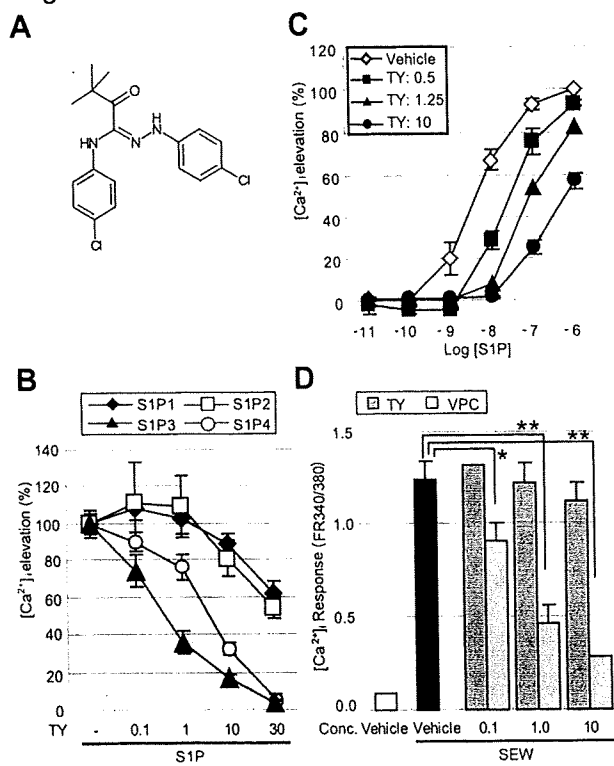


Fig.2

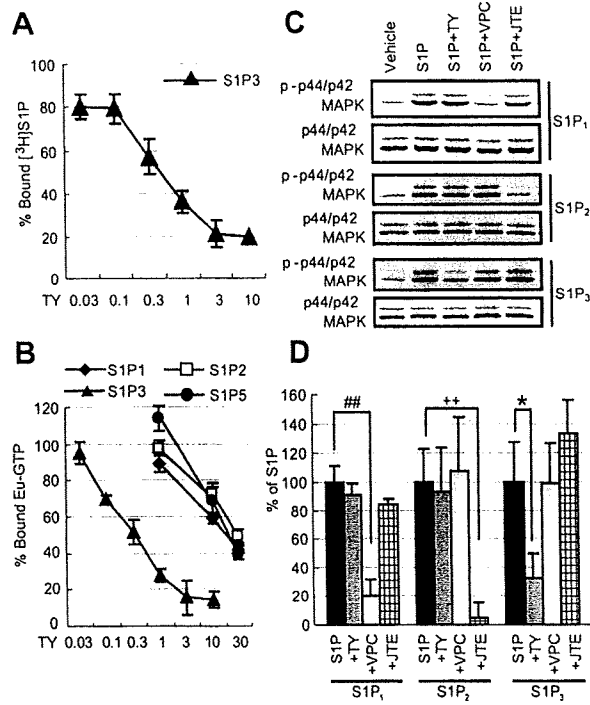


Fig.3

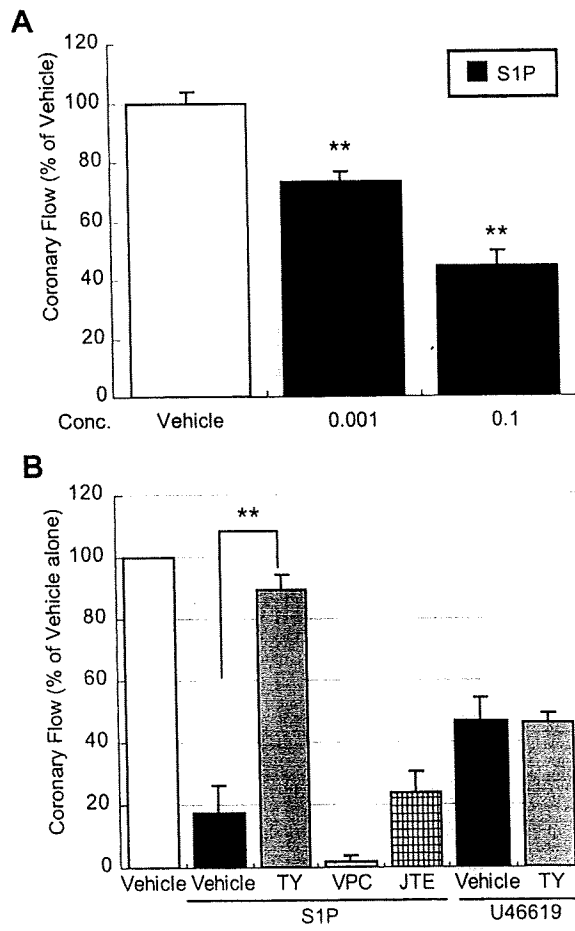


Fig.4

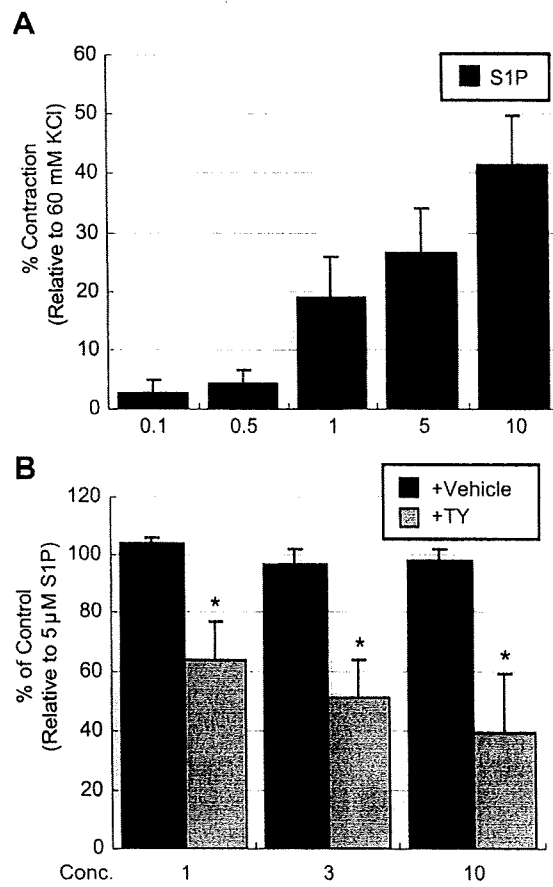




Fig.5

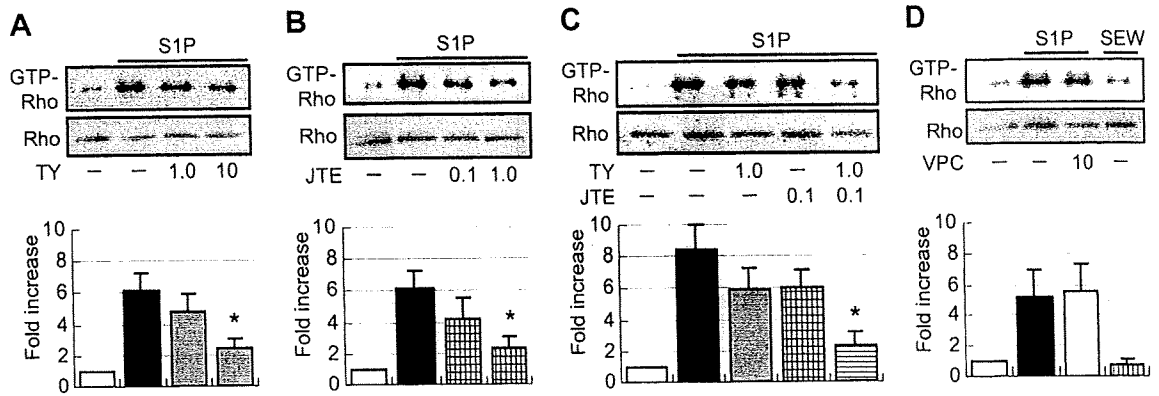


Fig.6

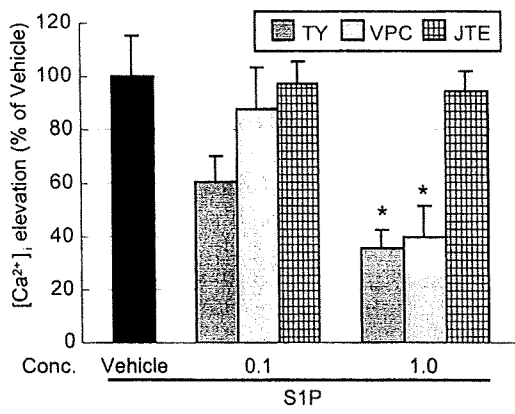


Fig.7

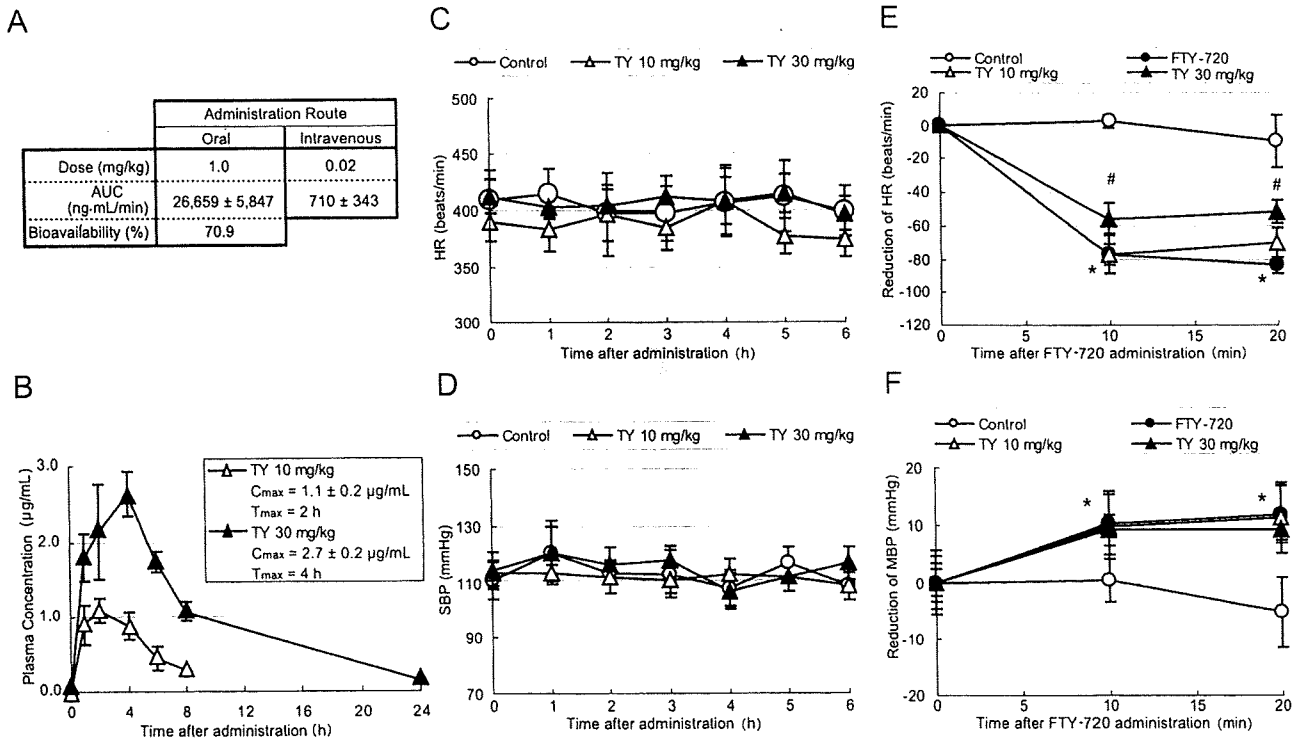


Fig.8

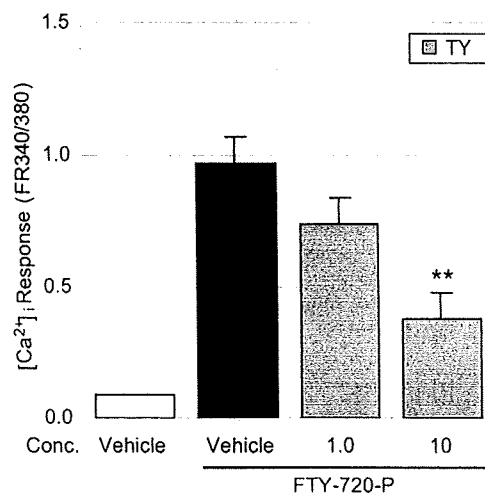
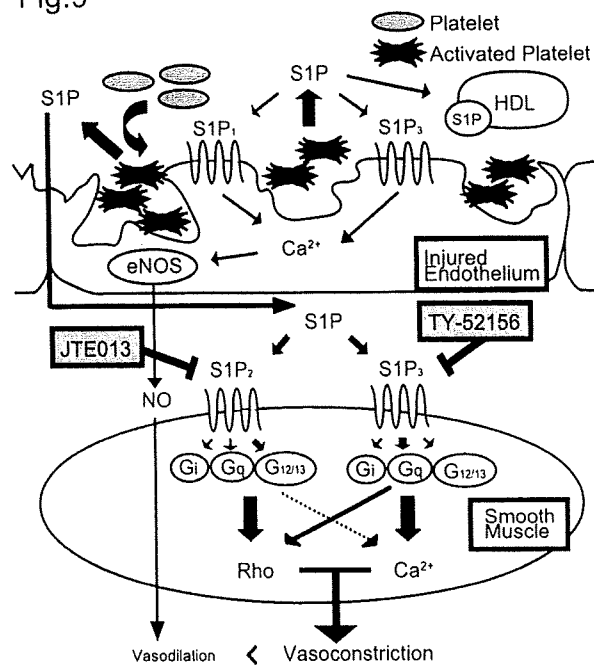


Fig.9



Scientific section designation: VASCULAR BIOLOGY

**Apelin induces enlarged and non-leaky blood vessels for functional recovery from ischemia**

Hiroyasu Kidoya<sup>1</sup>, Hisamichi Naito<sup>1</sup>, and Nobuyuki Takakura<sup>1</sup>

<sup>1</sup>Department of Signal Transduction, Research Institute for Microbial Diseases, Osaka University, 3-1 Yamada-oka, Suita, Osaka 565-0871, Japan.

To whom correspondence should be addressed to Nobuyuki Takakura, M.D. and Ph.D.

e-mail : [ntakaku@biken.osaka-u.ac.jp](mailto:ntakaku@biken.osaka-u.ac.jp) [N.T.]

TEL: 81-6-6879-8312,

FAX: 81-6-6879-8314

**Running title:** Functional blood vessel formation by apelin

**Key words:** Angiogenesis, apelin, APJ, ischemia, lumen size, vascular maturation, endothelial permeability, VE-cadherin

The online version of this article contains a data supplement.

## **ABSTRACT**

The efficacy of therapeutic angiogenesis for revascularization in ischemia utilizing genes, proteins and cells has been established. For further improvement, processes allowing enlargement of the luminal cavity to facilitate efficient blood flow need to be facilitated. Recently we found that expression of APJ and its specific ligand, apelin, is seen in endothelial cells (ECs) when angiogenesis is taking place during embryogenesis. Apelin-deficient mice are viable but have narrow intersomitic vessels during embryogenesis and narrow blood vessels in the trachea and skin after birth. Apelin induces the formation of larger cords of ECs, mainly mediated by cell-cell aggregation, resulting in the generation of larger blood vessels. Here we report that transgenic overexpression of apelin in keratinocytes induces enlarged but not leaky blood vessels in the dermis. In the hind limb ischemia model, apelin together with VEGF effectively induced functional vessels larger than with VEGF alone. Endogenous apelin is required for the suppression of VEGF-, histamine- or inflammation-induced vascular hyperpermeability. Apelin inhibited the down-modulation of VE-Cadherin by VEGF, resulting in suppression of hyperpermeability. Our results suggest apelin efficacy for therapeutic angiogenesis.

## INTRODUCTION

Vascular stenosis in large arteries caused by atherosclerosis, inflammatory processes and other events can lead to ischemia in different tissues and organs. Ischemia compromises microvascular function by damaging vascular endothelial cells (ECs), resulting in the reduction of functional capillaries and progression of ischemic ulceration and gangrene. Therefore, therapeutic angiogenesis is essential for restoration of blood flow to ischemic tissues and organs. Local administration of genes encoding pro-angiogenic factors such as vascular endothelial growth factor-A (VEGF), basic fibroblast growth factor (bFGF, FGF2), and hepatocyte growth factor (HGF), has been undertaken to manage patients with severe myocardial ischemia<sup>1,2</sup> or critical limb ischemia<sup>3,4</sup> refractory to conventional therapies. It has been reported that therapy with such genes enhanced collateral circulation by promoting angiogenesis in patients with critical limb ischemia disease.<sup>5,6</sup> In particular, gene therapy using the FGF1 expression plasmid NV1FGF resulted in a good outcome in patients with critical limb ischemia in Phase I and II trials.<sup>7</sup> However, it remains uncertain whether the administration of a single proangiogenic factor is sufficient to promote the formation of mature vessels that can provide adequate blood flow to ischemic lesions. Indeed, single gene administration of VEGF, bFGF, or HGF failed to demonstrate significant benefits in early Phase I and II human clinical trials.<sup>8-10</sup>

In the process of angiogenesis, proliferation and migration of ECs are required; subsequently EC-to-EC sealing is induced by tight junction formation and finally newly-developed blood vessels are stabilized by adhesion to mural cells such as pericytes or smooth muscle cells. These processes are not regulated by a single molecule but coordinately by several angiogenic factors.<sup>11,12</sup> Therefore, excessive amounts of one single proangiogenic factor, ignoring the balance between pro-angiogenic and anti-angiogenic factors, may induce disorganized blood vessels as observed in the tumor environment. Indeed, some reports suggest that excessive VEGF expression induces pathological and immature vessel formation



consisting of nascent capillaries, resulting in plasma leakage and tissue edema.<sup>13-15</sup> Therefore, it is suggested that therapeutic angiogenesis should be controlled by means of angiogenesis as observed *in vivo* and especially that regulation of stabilization and maturation processes is required for induction of functional blood vessel formation.

Combination gene therapy with several growth factors is a rational approach to creating more stable vessels for functional improvement in ischemic tissue. Among such factors, Angiopoietin1 (Ang1), a ligand for Tie2 on ECs, plays a critical role in promoting adhesion between mural cells and ECs, resulting in stabilization and enlargement of blood vessels.<sup>16-18</sup> Co-administration of VEGF and Ang1 modified angiogenesis and reduced vascular permeability in the skin of transgenic mice and in ischemic hind limb models.<sup>19-21</sup> These combination gene therapies are currently being examined in animal models in preparation for translation to clinical human therapy.<sup>22</sup> Thus, identification and utilization of maturation factors is required to achieve optimal therapeutic angiogenesis.

Apelin has been identified as the endogenous ligand of the G protein-coupled receptor APJ.<sup>23</sup> Apelin and APJ mediate a wide range of physiological actions including angiogenesis,<sup>24-27</sup> heart contractility and blood pressure regulation,<sup>29</sup> appetite and drinking behavior,<sup>30</sup> immune responses,<sup>31</sup> and other effects.<sup>32,33</sup> Apelin and APJ are expressed on ECs of the newly developing blood vessels during angiogenesis<sup>24</sup> and it has been reported that apelin expression is induced by hypoxia in ECs.<sup>26</sup> *In vitro* analysis revealed that apelin stimulates proliferation, migration, and tube formation of ECs.<sup>28,34</sup> Recently, we reported that apelin-deficient mice are viable but have narrow intersomitic vessels during embryogenesis and narrow blood vessels in the trachea and skin after birth. Apelin induces larger cords of ECs mainly mediated by cell-cell aggregation, resulting in formation of enlarged blood vessels.<sup>24</sup> Apelin expression is induced by the stimulation of Tie2 on ECs and we found that Ang1-mediated vascular enlargement<sup>35</sup> was abrogated in apelin-deficient mice.<sup>24</sup> Moreover, it has been reported that apelin deficiency significantly impaired retinal vascularization in the

early postnatal period.<sup>25</sup> Taken together, these data support the notion that the apelin/APJ pathway is important for vascular formation, especially for regulating caliber size of blood vessels to facilitate lumen enlargement.<sup>18,24</sup>

In the present study, we generated transgenic mice expressing apelin in the epidermis under the transcriptional control of the K14 promoter and observed the *in vivo* effects of apelin on blood vessel caliber size regulation. Moreover, we also studied the effects of apelin induction together with VEGF on functional recovery from ischemia in the mouse hind limb ischemia model. Furthermore, we analyzed the precise mechanism of how apelin induces non-leaky blood vessels associated with EC-to-EC junction fidelity mediated by VE-Cadherin.

## **METHODS**

### **Animals**

ICR and C57BL/6 mice were purchased from Japan SLC. The pK14-apelin-pA plasmid was generated by inserting the coding region of mouse apelin cDNA into the pK14-pA plasmid.<sup>36</sup> We generated K14-apelin transgenic mice according to standard methods.<sup>37</sup> We identified transgenic offspring by PCR of tail genomic DNA using forward (5'-GCC TGT GGG TGA TGA AAG CC-3') and reverse (5'-GGT CCA GTC CTC GAA GTT CT-3') primers. Three independent K14-apelin TG lines were backcrossed with wt C57BL/6 mice. Generation of apelin<sup>-/-</sup> mice was described previously.<sup>24</sup> Animals were housed in environmentally controlled rooms of the animal experimentation facility at Osaka University. All experiments were carried out under the guidelines of Osaka University Committee for animal and recombinant DNA experiments and were approved by the Osaka University institutional review board.

### **Quantitative real-time PCR analysis**

Total RNA was extracted from cells and tissues using the RNeasy Plus Mini kits (QIAGEN) and transcribed into cDNA using Exscript RT Reagent kits (Takara) according to the manufacturer's protocol. Primers for APJ, apelin, and GAPDH were previously described.<sup>24</sup> Real-time PCR analysis was performed by Platinum SYBR Green qPCR SuperMix-UDG (Invitrogen). The levels of PCR products were monitored with Mx3000P QPCR System (Stratagene). The baseline and threshold were adjusted according to the manufacturer's instructions. The relative abundance of transcripts were normalized using either the expression level of GAPDH mRNA or CD31 mRNA.

### **Western blot analysis**

The human VE-cadherin expression vector was a kind gift of Dr. Fukuhara (NCVC, Osaka, Japan). Lipofectamine Plus reagent (Invitrogen Life Technologies) was used to transfect cells

with this plasmid. Cell surface and cytoplasmic VE-cadherin expression by HUVECs was analyzed using a Mem-Per Reagent kit (Thermo) according to the manufacturer's protocol. Immunoblotting was performed to detect expression of VE-cadherin, N-cadherin, apelin, VEGF and GAPDH. Total cell lysates (2 µg total protein) were heated for 2 min at 95°C and then loaded onto SDS-polyacrylamide gels. Proteins were electrophoretically transferred onto polyvinylidene difluoride membranes, blocked with 5% nonfat dry milk, and subsequently incubated with anti-VE-cadherin, -N-cadherin (BD Bioscience), -apelin<sup>27</sup> (a gift from Takeda Pharmaceutical Company), -VEGF (Santa Cruz Biotechnology) or -GAPDH Abs (CHEMICON) according to the manufacturer's protocol. Proteins were detected with horseradish peroxidase-conjugated anti-mouse, anti-rabbit (DAKO), or anti-rat secondary Ab (Biosource) and ECL reagents (Amersham). In all experiments, the blots were scanned with an imaging densitometer LAS-3000 mini (Fujifilm). Predetermined molecular weight standards were used as markers. Protein concentration was measured by the protein assay dye reagent (BioRad) with BSA as a standard.

### **Immunostaining and lectin staining**

Sections from back skin and ears of K14-apelin Tg and wt mice were stained with anti-mouse CD31 antibody (PharMingen), anti-mouse APJ antibody<sup>24</sup> or anti-mouse apelin antibody<sup>24</sup>. The procedure for tissue preparation and staining was as previously reported.<sup>38</sup> HUVECs (Kurabo) were cultured in Humedia EG2 as described.<sup>24</sup> HUVECs were grown to confluence, serum starved, and stimulated with various factors. The cells were then fixed with 4% paraformaldehyde and permeabilized by 0.1% Triton X-100, labeled with anti-VE-cadherin antibody (BD Bioscience) and anti-p120-catenin antibody (Cosmobio), and visualized with AlexaFluor 488-conjugated goat anti-rat IgG and AlexaFluor 546-conjugated goat anti-mouse IgG (Molecular Probes). F-actin was stained with TRITC-conjugated Phalloidin (Sigma). Nuclear staining was performed using Hoechst 33258 (Sigma) or TOPRO3 (Invitrogen).